Scientific Research Journal,
Vol 20, Special Issue (2023) 113-125
https://doi.org/10.24191/srj.v20is.23308

Influence of Fe^{3+} Ion Substitution on Structural, Magnetic Properties and Magnetoresistance Effect of $Pr_{0.75}Na_{0.05}K_{0.20}MnO_3$ System

Siti Sumaiyah Sheikh Abdul Aziz[1,*], Norazila Ibrahim[2], Zakiah Mohamed[2], Rozilah Rajmi[3]

[1]Faculty of Applied Sciences, Universiti Teknologi MARA (UiTM), Cawangan Perak, Kampus Tapah, 35400 Tapah Road, Perak, Malaysia
[2]Faculty of Applied Sciences, Universiti Teknologi MARA (UiTM), 40450 Shah Alam, Selangor, Malaysia
[3]Faculty of Applied Sciences, Universiti Teknologi MARA (UiTM), Cawangan Perlis, Kampus Arau, 02600 Arau, Perlis, Malaysia

**Corresponding Author's E-mail: sumaiyahaziz@uitm.edu.my*

Received: 26 July 2023
Accepted: 18 October 2023
Online First: 27 October 2023

ABSTRACT

The effects of partial substitution of Fe at the Mn site on structural, magnetic, and electrical properties of monovalent doped $Pr_{0.75}Na_{0.05}K_{0.20}Mn_{0.95}Fe_{0.05}O_3$ manganite prepared by the solid-state method were investigated. X-ray Diffractometer, AC Susceptibility, and four point probe measurements were used to characterize the structural, magnetic, and electrical properties. The sample crystallized in an orthorhombic structure with a Pnma space group. The sample exhibited ferromagnetic (FM) to paramagnetic (PM) transition behaviour with Curie Temperature, T_C value of 121.5 K. From the resistivity versus temperature analysis, the sample exhibited insulating behaviour over entire temperature from 30 K - 300 K. Fe substitution exhibited high magnetoresistance (MR %) value at low temperature region, indicating the extrinsic mechanism of MR effect.

Keywords: Structural; Magnetic; Resistivity; Magnetoresistance

INTRODUCTION

Manganite materials with $A_{1-x}B_xMnO_3$ (A =La, Pr, Nd, B = Na, K) [1–3] have emerged as one of the most intriguing research topics due to their unique properties such as electrical and magnetic properties as well as colossal magnetoresistance (CMR) [4–6]. Furthermore, such properties can be considered for a new class of electronic devices based on the MR effect [7], which predicted an increase in wide applications areas such in consumer, automotive, medical, industrial, and other applications [8]. A wide range of studies has been conducted, focusing on various methods and chemicals [9] for improving the magnetic, electrical, and dielectric properties of these materials, which may be potential candidates for industrial applications such as spintronic-based devices [4, 5, 10], magnetic sensors [4], non-volatile memory elements [10], and supercapacitor electrodes. Thus, the tuneable properties exhibited by manganites make them highly attractive candidates for utilisation in various applications which also depending on few factors such as temperature and doping used in the investigation [9, 11].

Manganites exhibit tuneable electrical and magnetic properties by doping at the Mn site [12, 13]. Such properties directly affected the properties of the MnO_6 octahedral and the Mn^{3+}- O^{2-}-Mn^{4+} network [14]. In addition, several studies have been conducted to investigate the effect of doping at the Mn-site on the physical properties of manganites, such as in $Pr_{0.67}Sr_{0.16}Ca_{0.17}Mn_{0.75}Fe_{0.25}O_3$ [3], $La_{0.7}Ca_{0.3}Mn_{1-x}Cr_xO_3$ [4], and $Pr_{0.67}Ba_{0.22}Sr_{0.11}Mn_{1-x}Ti_xO_3$ [15]. According to studies, different substitutions of manganite systems exhibit different mechanisms and properties [9,16,17]. Among that, Fe substitution was reported to contribute to mixed phases of AFM clusters in the FM matrix [18,19]. As a result, it is intriguing to investigate the effect of Fe in $Pr_{0.75}Na_{0.05}K_{0.20}MnO_3$ manganites.

Interestingly, $Pr_{0.75}Na_{0.05}K_{0.20}MnO_3$ exhibit the highest value of ferromagnetic to paramagnetic transition temperature, T_C ~ 116 K, as compared to another sample as reported by previous study [2]. Thus, substitution of Fe^{3+} at Mn-sites will play an important role in magnetic, electrical properties and magnetoresistance in $Pr_{0.75}Na_{0.05}K_{0.20}MnO_3$ manganite due to the presence of mixed phases consisting of AFM clusters in the FM matrix.

METHODOLOGY

The solid-state method was used to synthesize $Pr_{0.75}Na_{0.05}K_{0.20}Mn_{0.95}Fe_{0.05}O_3$ from high purity (99.99 %) of Pr_6O_{11}, Na_2CO_3, K_2CO_3, Fe_2O_3, and MnO_2 in the appropriate stoichiometric ratio. With two intermediate grindings, the materials were thoroughly mixed, ground, and calcined for 24 h at 950 ℃. Then, the mixtures were reground and pressed into pellets under 5 tons of pressure, with diameter of 13 mm and thickness of around 3 mm. The samples were then sintered at 1100 ℃ for 36 h. The morphology of the sample was examined using a scanning electron microscope (SEM) (LEO model 982 Gemini) at a magnification of 10K. The elemental composition was determined using the energy dispersive X-ray (EDX) technique. AC susceptibility was set up to measure the magnetic properties of the samples from 30 K to 300 K. The electrical resistivity and magnetoresistance (MR) behaviors of samples were investigated using the standard four-point probe technique (Janis model CCS 350ST cryostat) at temperatures ranging from 30 K to 300 K in external magnetic fields of around 0.8 T.

RESULTS AND DISCUSSION

Structural Properties

Figure 1 (a) depicts the XRD pattern for a $Pr_{0.75}Na_{0.05}K_{0.20}Mn_{0.95}Fe_{0.05}O_3$ sample. As can be seen, the sample has a single phase with no discernible secondary phase. The Rietveld technique was used to refine the data using the EXPGUI and GSAS programmes. All diffraction peaks were indexed in an orthorhombic perovskite structure with the space group pmna (No.62) as shown in Figure 1 (b). This result aligns with the published data for the undoped sample [2, 20] which indicated a good quality data. The structural parameters from the Rietveld refinement for $Pr_{0.75}Na_{0.05}K_{0.20}Mn_{0.95}Fe_{0.05}O_3$ manganite are listed in Table 1. The tolerance factor (τ) was measured to determine the stability of the structure was discovered to have a similar value (0.9451) to the parent compound of $Pr_{0.75}Na_{0.05}K_{0.20}MnO_3$ as stated by previously published data [20]. The results showed that the Fe substitution at Mn-site had no effect on the structure of the investigated sample could be due to similar ionic radius of Fe^{3+} and Mn^{3+} ions (0.645 Å) [21,22].

Table 1: Lattice Parameters; Unit Cell Volume, V; Tolerance Factor, τ and χ2; for $Pr_{0.75}Na_{0.05}K_{0.2}Mn_{0.95}Fe_{0.05}O_3$

Parameter	
Symmetry	Orthorhombic
Space Group	Pnma
a (Å)	5.4422 (3)
b (Å)	7.6844 (2)
c (Å)	5.4457 (3)
V (Å^3)	5.4337 (2)
χ^2	1.272
τ	0.9451

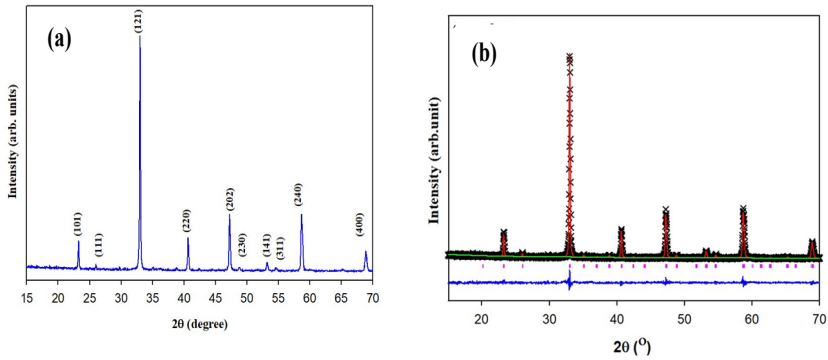

Figure 1: (a) XRD diffraction patterns and (b) Rietveld X-ray diffraction pattern refinement for $Pr_{0.75}Na_{0.05}K_{0.2}Mn_{0.95}Fe_{0.05}O_3$ at room temperature

Morphology Properties

SEM micrographs of the $Pr_{0.75}Na_{0.05}K_{0.20}Mn_{0.95}Fe_{0.05}O_3$ with ten thousand (×10k) magnification is shown in the inset of Figure 2 which shows the grains are irregular in shape and size. All the elements are shown in Figure 2 examined by the energy dispersive X-ray (EDX), which proved the existence of all elements in the compound.

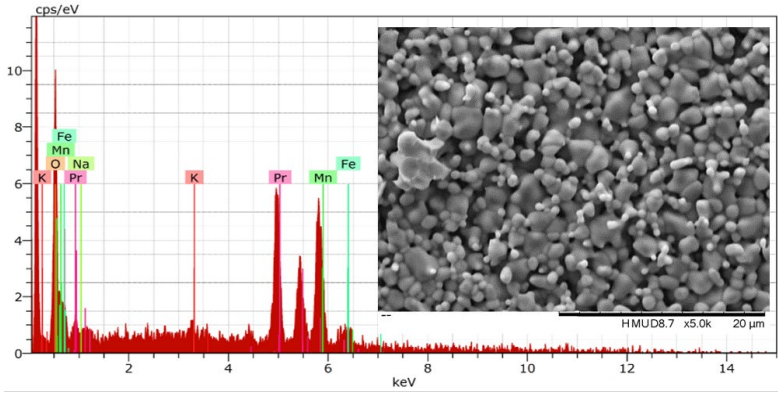

Figure 2: EDX spectra for the $Pr_{0.75}Na_{0.05}K_{0.2}Mn_{0.95}Fe_{0.05}O_3$. Inset: SEM image for the $Pr_{0.75}Na_{0.05}K_{0.2}Mn_{0.95}Fe_{0.05}O_3$ with a magnification of 5k

Magnetic Properties

As shown in Figure 3(a), the real part of the AC susceptibility measurements versus temperature of $Pr_{0.75}Na_{0.05}K_{0.20}Mn_{0.95}Fe_{0.05}O_3$ sample exhibits a ferromagnetic to paramagnetic (FM-PM) phase transition with the increase of temperature. The Curie temperature (T_C) was observed at 121.5 K, which determined by the minimum temperature curves of $d\chi/dt$ versus temperature shown in the inset Figure 3(a). According to Aziz *et al.*[20], the parent compound has a higher T_C value (140.7 K) compared to the studied sample [20]. The significant decrease in T_C could be attributed to a weakening of ferromagnetic (FM) interaction caused by an enhancement of antiferromagnetic (AFM) ordering with Fe substitution [3]. A few reports similar finding regarding Fe substitution at Mn-site, suggesting that the weakening of FM interaction could also be due to the reduction of the Mn^{3+}/Mn^{4+} ratio [23, 24].

In order to gain more in-depth into the magnetic properties within the paramagnetic (PM) region, a graph illustrating the inverse of χ' plotted against temperature (T) was generated, as depicted in Figure 3(b). The linear behaviour of the inverse susceptibility suggests that the data follows to the Curie-Weiss law which defined by $\chi = C/(T-\theta_P)$ where χ, C and θ_P represent the magnetic susceptibility, Curie constant and Weiss temperature, as shown by the fitting curve (solid red line) depicted in the Figure 3(b).

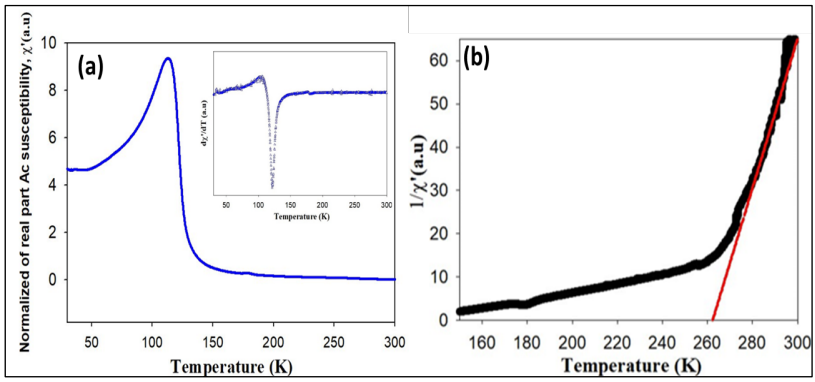

Figure 3: (a) The real part of AC susceptibility (χ') and (b) the inverse magnetic susceptibility (χ^{-1}) versus temperature for $Pr_{0.75}Na_{0.05}K_{0.2}Mn_{0.95}Fe_{0.05}O_3$. Inset: The plot of $d\chi'/dt$ versus temperature for $Pr_{0.75}Na_{0.05}K_{0.2}Mn_{0.95}Fe_{0.05}O_3$

Electrical Properties

As previously reported, the $Pr_{0.75}Na_{0.05}K_{0.2}MnO_3$ compound exhibited a metal insulator (M-I) transition at transition temperature (T_{MI}) of 122 K for 0 T and 0.8 T of applied field [20]. In contrast, substitution of Fe in $Pr_{0.75}Na_{0.05}K_{0.20}Mn_{0.95}Fe_{0.05}O_3$ sample exhibits insulating behavior over the whole temperature range from 30 K to 300 K for 0 T field. The observed behaviour may be explained by the dominant effect of the super-exchange (SE) mechanism, which involves Fe^{3+}- Fe^{3+}, Mn^{3+}- Mn^{3+} and Mn^{4+}- Mn^{4+} [24]. Furthermore, other research stated a similar suggestion such as Fe^{3+} doped in $Pr_{0.67}Sr_{0.16}Ca_{0.17}Mn_{0.75}Fe_{0.25}O_3$ manganite and reported that Fe^{3+} ion does not participate in the double exchange (DE) mechanism [3]. In addition, the resistivity decreases as the temperature increases and is almost constant at high temperature above 100 K, as depicted in Figure 4. This phenomenon can be attributed to the delocalization of charge carriers inside the sample as a result of the increased energy levels caused by the temperature increase [3].

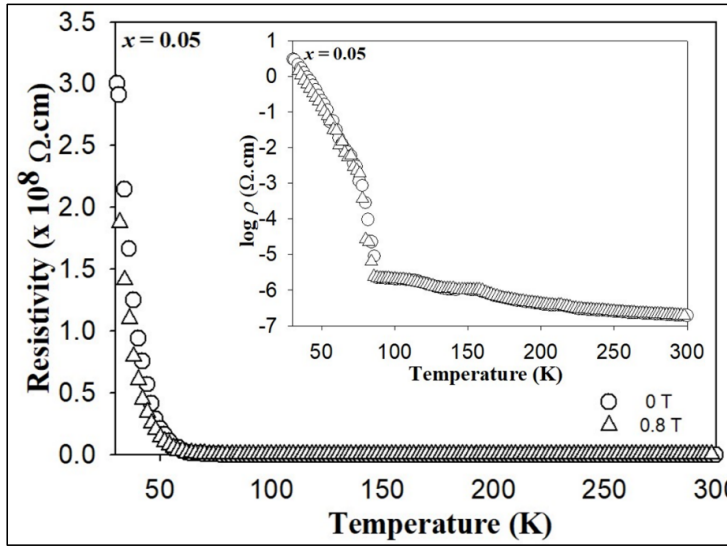

Figure 4: Temperature dependence of resistivity for $Pr_{0.75}Na_{0.05}K_{0.2}Mn_{0.95}Fe_{0.05}O_3$. Inset show the log ρ vs T for $Pr_{0.75}Na_{0.05}K_{0.2}Mn_{0.95}Fe_{0.05}O_3$.

Under a 0.8 T magnetic field, however, the resistivity slightly reduced supported by the graph of log ρ versus temperature (in the inset of Figure 4), resulting in the magnetoresistance (MR) effect. The MR effect which calculated using equation MR (%) $=(\rho(0,T)-\rho(H,T))/\rho(0,T) \times 100\%$, where ρ(0,T) and ρ(H,T) represent the resistivity for 0 T and 0.8 T fields [25–27]. The MR % is high at low temperatures, as shown in Figure 5, indicating the extrinsic mechanism of MR effect. This behaviour is indicated that applying an external magnetic field aligns disordered Mn spins in grain boundary regions which enhanced the spin-polarised tunnelling (SPT) mechanism between grains [27,28]. The findings are consistent with a prior study that reported a similar suggestion [27,29,30].

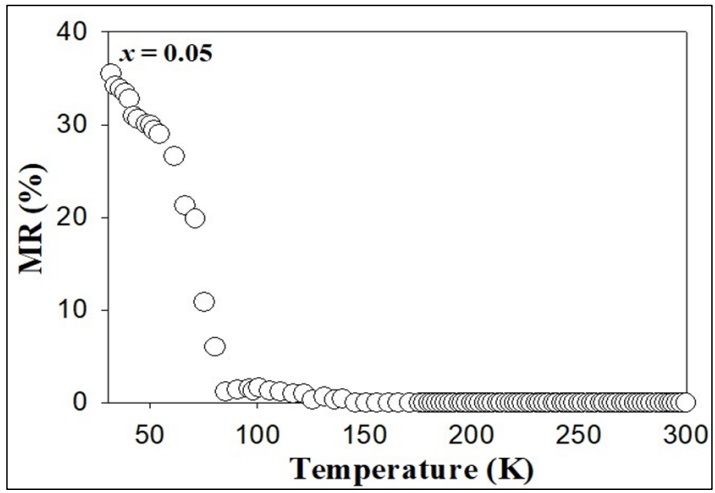

Figure 5: Temperature dependence of Magnetoresistance (MR) of $Pr_{0.75}Na_{0.05}K_{0.2}Mn_{0.95}Fe_{0.05}O_3$

CONCLUSION

In summary, $Pr_{0.75}Na_{0.05}K_{0.20}Mn_{0.95}Fe_{0.05}O_3$ compound crystallized in an orthorhombic structure with a Pnma space group and exhibited ferromagnetic (FM) to paramagnetic (PM) with a Curie temperature of 121.5 K. The linear relationship of the inverse magnetic susceptibility, as described by the Curie-Weiss law, is observed. The resistivity data of the compound exhibits insulating behaviour when Fe is substituted across all temperatures and reveals a decrease in resistivity as the temperature increases. Magnetoresistance (MR) versus temperature graphs demonstrated that Fe substitution elevated MR at low temperatures, revealing that the extrinsic MR effect dominated.

ACKNOWLEDGEMENTS

This work was partially funded by the Ministry of Higher Education (MOHE), Malaysia, and Universiti Teknologi MARA for supporting this project under the Fundamental Research Grant Scheme (FRGS) [Ref: 600-

IRMI/FRGS 5/3 (330/2019)].

REFERENCES

[1] S. Bouzidi, M. A. Gdaiem, A. Dhahri, J. Dhahri & E. K. Hlil, 2020. Charge transport mechanism and percolation model in $La_{0.75}Ca_{0.25-x}Na_xMnO_3$ ($0 \leq x \leq 0.10$) manganites. *Journal of Materials Science: Materials in Electronics*, 31 (14), 11548–11559, doi: 10.1007/s10854-020-03703-1.

[2] R. Rozilah, N. Ibrahim, Z. Mohamed, A. K. Yahya, N. A. Khan & M. N. Khan, 2017. Inducement of ferromagnetic-metallic phase in intermediate-doped charge-ordered $Pr_{0.75}Na_{0.25}MnO_3$ manganite by K+ substitution. *Physica B: Condensed Matter*, 521, 281–294, doi: 10.1016/j.physb.2017.07.001.

[3] Z. Mohamed, A. Ben Hassen, A. Somrani & E. K. Hlil, 2022. Structural, magnetic and electrical properties of new perovskite $Pr_{0.67}Sr_{0.16}Ca_{0.17}Mn_{0.75}Fe_{0.25}O_3$ material. *Journal of Low Temperature Physics,* 209 (2), 198-212, doi: 10.1007/s10909-022-02772-2.

[4] N. Kumar, H. Kishan, A. Rao & V. P. S. Awana, 2010. Structural, electrical, magnetic, and thermal studies of Cr-doped $La_{0.7}Ca_{0.3}Mn_{1-x}Cr_xO_3$ ($0 \leq x \leq 1$) manganites. *Journal of Applied Physics*, 107 (8), 0–6, doi: 10.1063/1.3342462.

[5] A. Swain, P. S. Anil Kumar & V. Gorige, 2019. Electrical conduction mechanism for the investigation of charge ordering in $Pr_{0.5}Ca_{0.5}MnO_3$ manganite system. *Journal of Magnetism and Magnetic Materials,* 485, 358–368, doi: 10.1016/j.jmmm.2019.04.097.

[6] P. G. R. Achary, S. Behera, R. N. P. Choudhary & S. K. Parida, 2021. Structural, dielectric and electrical properties of cerium-modified strontium manganite ceramics. J*ournal of Materials Science: Materials in Electronics,* 32 (5), 5738–5754, doi: 10.1007/s10854-021-05295-w.

[7] S. K. Estemirova, V. Y. Mitrofanov, S. A. Uporov & R. I. Gulyaeva,

2020. Effect of cation substitution on structural, magnetic and magnetocaloric properties of $(La_{0.7}Eu_{0.3})_{0.75}Sr_{0.25}Mn_{0.9}(Me)_{0.1}O_3$ (Me = Co, Ti). *Journal of Magnetism and Magnetic Materials,* 502, 166593, doi: 10.1016/j.jmmm.2020.166593.

[8] F. Grown, S. Substrate, I. Mocvd & N. Žurauskien, 2023. Magnetoresistance and magnetic relaxation of La-Sr-Mn-O magnetoresistance and magnetic relaxation of La-Sr-Mn-O films grown on Si/SiO2 substrate by pulsed injection MOCVD. *Sensors,* 23(12), 5365.

[9] H. Belmabrouk & T. Alharbi, 2023. Dielectric properties and conduction mechanism of $La_{0.7}Sr_{0.25}Na_{0.05}Mn_{0.95}Al_{0.05}O_3$ perovskite manganite. *Journal of Taibah University for Science,* 7(1), 0–11, doi: 10.1080/16583655.2023.2204809.

[10] K. Gadani, M. J. Keshvani. D. Dhruv, H. Boricha, K. N. Rathod, P. Prajapati, A. D. Joshi, D. D. Pandya, N. A. Shah & P. S. Solank, 2017. Low field magnetoelectric and magnetotransport properties of sol–gel grown nanostructured $LaMnO_3$ manganites. *Journal of Alloys and Compounds,* 719, 47–57, doi: 10.1016/j.jallcom.2017.05.165.

[11] B. Biswas, R. Nag, S. Mondal, M. H. Khan, M. Debnath, S. Taran & S. Pal, 2023. Magnetic field dependent metal insulator transition by monovalent doping (Na^+) in $PrMnO_3$: Investigation through structural, magnetic and transport properties. *Physica B: Condensed Matter,* 652, 414664, doi: 10.1016/j.physb.2023.414664.

[12] I. O. Troyanchuk, M. V. Bushinsky, D. V. Karpinsky, N. V. Tereshko, V. M Dobryansky, D. M. Tobbens, V. Sikolenko, V. Efimov, 2015. Magnetic interactions in $La_{0.7}Sr_{0.3}Mn_{1-x}Me_xO_3$ (Me=Ga, Fe, Cr) manganites. *Journal of Magnetism and Magnetic Materials,* 394, 212–216, doi: 10.1016/j.jmmm.2015.06.046.

[13] Y. Li, J. Miao, Y. Sui, Z. Lü, Z. Qian & W. Su, 2006. Phase separation, low-field magnetic and transport properties of $Pr_{0.75}Na_{0.25}Mn_{0.9}Fe_{0.1}O_3$. *Journal of Magnetism and Magnetic Materials,* 305(1), 247–252, doi: 10.1016/j.jmmm.2006.01.009.

[14] B. Sudakshina, B. Arun, K. D. Chandrasekhar, H. D. Yang & M. Vasundhara, 2018. Structural and magnetic properties of $Nd_{0.67}Ba_{0.33}MnO_3$ manganites with partial replacement of Fe and Cu at Mn-site. *Physica B: Condensed Matter,* 539, 14–20, doi: 10.1016/j.physb.2018.04.002.

[15] K. Snini, F. Ghribi, A. Ekicibil, M. Ellouze & L. El Mir, 2020. Structural, electrical properties and complex impedance analysis of $Pr_{0.67}Ba_{0.22}Sr_{0.11}Mn_{1-x}Ti_xO_3$ perovskites. *Journal of Materials Science: Materials in Electronics,* 31(23) 20657–20666, doi: 10.1007/s10854-020-04596-w.

[16] I. Ouni, H. B. Khlifa, R. M'nassri, M. M. Nofal, E. M. A. Dannoun, H. Rahmouni, K. Khirouni, A. Cheikhrouhou, 2021. Transport properties and dielectric response of $Pr_{0.8}Na_{0.2-x}K_xMnO_3$ (x = 0, 0.05, 0.1, 0.15 and 0.2) ceramics synthesized by sol–gel method. *Applied Physics A,* 127 (8), 631, doi: 10.1007/s00339-021-04760-x.

[17] S. Aydi, W. Chérif, F. Khammassi, A. J. M. Sales, N. M. Ferreira & N. Zouari, 2021. Microstructural properties, dielectric behaviour, conduction mechanism, impedance, and electrical modulus of $La_{0.65}Ca_{0.25}Sr_{0.1}MnO_3$ manganite. *Applied Physics A: Materials Science and Processing,* 127(12) 0–12, doi: 10.1007/s00339-021-05057-9.

[18] L. Joshi, V. Dayal, N. Rama & S. Keshri, 2009. Existence of Griffiths phase in $La_{0.67}Ca_{0.33}Mn_{0.93}Fe_{0.07}O_3$. *Journal of Alloys and Compounds,* 479 (1–2)879–882, doi: 10.1016/j.jallcom.2009.01.140.

[19] S. Ait Bouzid, M. Sajieddine, O. Mounkachi, E. Kebir Hlil, M. Mansori & A. Essoumhi, 2021. Influence of iron substitution on the ferromagnetic ordering and magnetic entropy variation in $La_{1-x}Na_xMn_{1-y}Fe_yO_3$ (x = 0.1, 0.2 and y = 0, 0.1). *Journal of Magnetism and Magnetic Materials,* 537, doi: 10.1016/j.jmmm.2021.168194.

[20] S. S. S. A. Aziz, N. Ibrahim, R. Rajmi & Z. T. Mohamed, 2022. Magnetic properties and evolution of magnetoresistance effect in $Pr_{0.75}Na_{0.05}K_{0.20}Mn_{1-x}Fe_xO_3$ with $0 \leq x \leq 0.04$. *Applied Physics A,* 128

(10), 940, doi: 10.1007/s00339-022-06075-x.

[21] K. Snini, F. Ben Jemaa, M. Ellouze & E. K. Hlil, 2018. Structural, magnetic and magnetocaloric investigations in $Pr_{0.67}Ba_{0.22}Sr_{0.11}Mn_{1-x}Fe_xO_3$($0 \leq x \leq 0.15$) manganite oxide. J*ournal of Alloys and Compounds,* 739, 948–954, doi: 10.1016/j.jallcom.2017.12.309.

[22] Y. Zhou, X. Zhu & S. Li, 2017. Structure, magnetic, electrical transport and magnetoresistance properties of $La_{0.67}Sr_{0.33}Mn_{1-x}Fe_xO_3$ (x=0–0.15) doped manganite coatings. *Ceramics International,* 43 (4) 3679–3687, doi: 10.1016/j.ceramint.2016.11.210.

[23] S. K. Estemirova, V. Y. Mitrofanov, S. A. Uporov & G. A. Kozhina, 2021. Magnetocaloric properties of Fe-substituted La–Sr-manganites. *Solid State Sciences,* 124 (14), 106806, doi:10.1016/j.solidstatesciences.2022.106806.

[24] A. Mounira, 2019. Effect of Fe substitution on the physical properties of $La_{0.62}Er_{0.05}Ba_{0.33}Mn_{1-x}Fe_xO_3$(x = 0.00, 0.05 and 0.15). *Journal of Superconductivity and Novel Magnetism,* 32 (2), 301–310, doi: 10.1007/s10948-018-4707-7.

[25] S. Solanki, D. Dhruv, H. Boricha, A. Zankat, K. N. Rathod, B. Rajyaguru, R. K. Trivedi, A. D. Joshi, S. Mukherjee, P. S. Solanki & N. A. Shah, 2020. Charge transport mechanisms and magnetoresistance behavior of $La_{0.6}Pr_{0.1}Ca_{0.3}MnO_3$ manganite. *Journal of Solid State Chemistry,* 288, 121446, doi: 10.1016/j.jssc.2020.121446.

[26] U. K. Sinha, B. Das & P. Padhan, 2020. Interfacial reconstruction in $La_{0.7}Sr_{0.3}MnO_3$ thin films: Giant low-field magnetoresistance. *Nanoscale Advances,* 2(7), 2792–2799, doi: 10.1039/d0na00287a.

[27] A. Pal, B. S. Nagaraja, K. J. Rachana, K. V. Supriya, D. Kekuda, A. Rao, C. R. Li & Y. K. Kuo, 2020. Enhancement of temperature coefficient of resistance (TCR) and magnetoresistance (MR) of $La_{0.67-x}RE_xCa_{0.33}MnO_3$ (x = 0, 0.1; RE = Gd, Nd, Sm) system via rare-earth substitution. *Materials Research Express*, 7(3), doi: 10.1088/2053-

1591/ab7c20.

[28] R. Rozilah, N. Ibrahim & A. K. Yahya, 2019. Inducement of ferromagnetic–metallic phase and magnetoresistance behavior in charged ordered monovalent-doped $Pr_{0.75}Na_{0.25}MnO_3$ manganite by Ni substitution. *Solid State Sciences,* 87, 64–80, doi: 10.1016/j.solidstatesciences.2018.11.005.

[29] N. Ibrahim & A. K. Yahya, 2021. Enhancement of extrinsic magnetoresistance behavior in $BiFeO_3$ doped $La_{0.8}Ag_{0.2}MnO_3$ ceramic. *Ceramics International,* 39 (1), S181–S184, 2013, doi: 10.1016/j.ceramint.2012.10.058.

[30] M. R. Lees, J. Barratt, G. Balakrishnan, D. M. Paul & C. D. Dewhurst, 1996. Low-temperature magnetoresistance and magnetic ordering in in $Pr_{1-x}Ca_xMnO_3$. *Journal of Physics: Condensed Matter,* 8(17), 2967–2979, doi: 10.1088/0953-8984/8/17/009.